PHYSICAL REVIEW D **83,** 114003 (2011)

Roles of axial anomaly on neutral quark matter with color superconducting phase

Zhao Zhang
School of Mathematics and Physics, North China Electric Power University, Beijing 102206, China

Teiji Kunihiro
Department of Physics, Kyoto University, Kyoto 606-8502, Japan
(Received 25 February 2011; published 1 June 2011)

We investigate the effects of the axial-anomaly term with a chiral-diquark coupling on the phase diagram within a two-plus-one-flavor Nambu-Jona-Lasinio model under the charge-neutrality and β-equilibrium constraints. We find that when such constraints are imposed, the new anomaly term plays a quite similar role as the vector interaction does on the phase diagram, which the present authors clarified in a previous work. Thus, there appear several types of phase structures with multiple critical points at low temperature T, although the phase diagrams with intermediate-T critical point(s) are never realized without these constraints even within the same model Lagrangian. This drastic change is attributed to an enhanced interplay between the chiral and diquark condensates due to the anomaly term at finite temperature; the u-d diquark coupling is strengthened by the relatively large chiral condensate of the strange quark through the anomaly term, which in turn definitely leads to the abnormal behavior of the diquark condensate at finite T, inherent to the asymmetric quark matter. We note that the critical point from which the crossover region extends to zero temperature appears only when the strength of the vector interaction is larger than a critical value. We also show that the chromomagnetic instability of the neutral asymmetric homogenous two-flavor color-superconducting phase is suppressed and can be even completely cured by the enhanced diquark coupling due to the anomaly term and/or by the vector interaction.

DOI: 10.1103/PhysRevD.83.114003 PACS numbers: 12.38.Aw, 11.10.Wx, 11.30.Rd, 12.38.Gc

I. INTRODUCTION

It is generally believed that the strongly interacting matter exhibits a rich phase structure in an extreme environment such as at high temperature and high baryon chemical potential. Experimentally, the Relativistic Heavy-Ion Collider and Large Hadron Collider may provide more information on this topic. Theoretically, some results have been already obtained on a sound basis: First, the lattice simulations of quantum chromodynamics (QCD) indicate that, for physical quark masses, the transition from the hadronic phase to the quark gluon plasma is a smooth crossover at finite temperature and vanishing baryon chemical potential [1,2], whereas in the low-temperature and very high density region, the techniques of perturbation QCD can be used and the color flavor locking (CFL) [3] phase is proved to be the ground state of QCD [4–7].

However, the above methods based on the first principle fail at the low temperature and moderate density region, due to the sign problem or the nonperturbative effect. Phenomenologically, such a region in the T-μ plane is more relevant to reality and hence interesting since it is directly related to the physics of compact stars. On that account, chiral models of QCD such as the Nambu-Jona-Lasinio (NJL) model [8–11] that embody the basic low-energy characteristics of QCD such as symmetry properties have been extensively used to explore the T-μ phase diagram of strongly interacting matter. In particular, such model calculations suggest that color superconducting (CSC) phase may occur at low temperature and large chemical potential (for reviews, see [12–15]). In addition, a popular result from the model studies is that the chiral phase transition always keeps first order at the low-temperature region [16–21]. Combined with the crossover transition confirmed by lattice QCD at zero baryon chemical potential, usually, a schematic T-μ phase diagram with one chiral critical point (CP) is widely adopted in the literature [22]. Such a CP may be located at relatively high temperature and low baryon chemical potential, which has attracted considerable attention as it is potentially detectable in heavy-ion experiments [23,24].

Generally, there is no reason to rule out the possibility that the QCD phase diagram may contain more than one chiral CP, especially when the chiral and diquark condensates are considered simultaneously; some rich structures with multiple CPs may be expected for the phase diagram owing to somehow enhanced interplay between the two types of condensates.[1] It has been shown on the basis of the NJL model that it is indeed the case [27–30]; the QCD phase diagram can admit multiple CPs when the repulsive

*zhaozhang@pku.org.cn
†kunihiro@ruby.scphys.kyoto-u.ac.jp

[1]Note that multiple critical points had also been found in two-flavor models of QCD without considering diquark paring [25,26].

vector interaction [27,28] or the charge-neutrality and β equilibrium [29] or both of these two ingredients [30] are included.[2] This is because the two ingredients act so as to enhance the competition between the chiral and diquark condensates and thus the would-be first-order boundary line in the low-temperature region of the T-μ plane can be turned into a smooth crossover or multiply-cut crossover lines with new CP(s). Indeed it has been found [30] that the number of the chiral CPs may vary from zero to four with the joint effect of these two ingredients. Moreover, the present authors have shown [30] that the vector interaction can effectively suppress the chromomagnetic instability [33] in the asymmetric homogeneous CSC phase.

It is noteworthy that a direct coupling term between the chiral and diquark condensates can be supplied by the axial anomaly [3,34,35], which thus might lead to a new CP in the low-temperature region, as first conjectured in [36] on the basis of an analysis using the Ginzburg-Landau (GL) theory in the chiral limit; see also subsequent detailed analyses [37,38] though still in the chiral limit. It is, however, to be noted that the GL theory assumes that both the diquark and chiral condensates are sufficiently small around the phase boundaries provided that the phase transitions are of second-order. In addition, the GL theory itself can not determine the coefficients in the action, and some microscopic model or theory is necessary for such a determination.

Recently, a microscopic calculation has been done [39] with the use of a three-flavor NJL model for massive quarks incorporating the axial-anomaly term with a form of a six-quark interaction [3,34,35,37], the coupling constant of which is denoted by K': It was claimed in [39] that the low-temperature CP can exist owing to the axial anomaly for an appropriate range of the model parameters even off the chiral limit but still with a flavor symmetry as in the GL approach in the chiral limit. It should be noticed, however, that the SU(3)-flavor symmetry may lead to a special type of CSC phase, i.e., the CFL phase, as is taken for granted in [36–39], which automatically satisfies the charge neutrality and β-equilibrium constraints.

Then one may suspect that the possible emergence of the new CP might be an artifact of such an ideal situation with the three-flavor symmetry. Nevertheless, it is a very interesting possibility that the axial anomaly-induced interplay between the chiral and diquark condensates would lead to a new CP in the low-temperature region. Thus it is worth exploring to see whether a new low-temperature CP is induced by the axial anomaly in a dynamical model of QCD by considering the realistic situation with the broken flavor symmetry by the hierarchical current-quark masses.

[2]Note that the renormalization group theory for deducing low-energy effective vertex favors the presence of the vector-type interaction [31,32].

We note that once the quark mass difference of different flavors is taken into account, it becomes a complicated dynamical problem to make the charge-neutrality and β-equilibrium constraints satisfied.

More recently, such a realistic calculation in the framework of a two-plus-one-flavor NJL model has been done by Basler *et al.* [40]; they have shown that such a new low-temperature CP is not found in such a model even with the axial-anomaly term, because an unusual interplay between the chiral and diquark condensates induced by the anomaly term actually leads favorably to the two-flavor color superconducting (2CSC) phase [41,42] rather than the CFL phase near the chiral phase boundary, even in the case with the equal quark mass limit [40].

It is worth emphasizing here that the constraints by the charge neutrality and β equilibrium are not taken into consideration in [39] nor [40] in contrast to [29,30] where various types of multiple-CP structures are found in the phase diagram. Thus, the following two questions arise naturally: Will the results found in [40] be altered or not when the charge-neutrality and β-equilibrium constraints and/or the vector interaction are taken into account? Or will the phase structure with multiple CPs found in [30] rather persist when taking into account the coupling between the chiral and diquark condensates induced by such a six-quark interaction? The main purpose of this paper is to answer these questions by incorporating the anomaly term that breaks the $U_A(1)$ symmetry as well as the vector interaction under the constraints of the charge neutrality and β equilibrium in the two-plus-one-flavor NJL model. The present work may be regarded as either an extension of Ref. [40] by incorporating the charge neutrality, β equilibrium, and the vector interaction, or an extension of Ref. [30] by including the K' interaction.

The main conclusion we reach is that the key results on the phase structure obtained in Refs. [29,30] persist even when the attractive K' interaction is incorporated. That is, there appear new CP(s) at the intermediate temperature owing to the charge-neutrality constraint and then the transition in the low-temperature region extending to zero T becomes a crossover when the strength of the vector interaction becomes larger than a critical value: Thus, the number of the CPs can be even more than two, depending on the values of some related coupling constants. Strikingly enough, we find that the interplay between the chiral and the diquark condensates induced by the anomaly term even acts toward realizing the multi-CP structure of the phase diagram under the neutrality and β-equilibrium constraints even without the help of the vector interaction. Accordingly, the results in Ref. [40] are modified by considering these constraints. The chiral boundary in the low-T region extending to zero T also remains first order in our case in the absence of the vector interaction, which shrinks and vanishes eventually as K' becomes large and exceeds a critical value.

We shall also examine the chromomagnetic (in)stability under the influence of the axial anomaly, as was done in [30]. It is well known that the asymmetric homogenous 2CSC phase suffers from the chromomagnetic instability. At zero temperature, the calculation based on the hard-dense-loop method [33] suggests that the Meissner mass squared of the 8th gluon becomes negative for $\frac{\delta\mu}{\Delta} > 1$ while the 4th–7th gluons acquire negative Meissner masses squared for $\frac{\delta\mu}{\Delta} > 1/\sqrt{2}$; here $\delta\mu$ and Δ denote the difference of the chemical potentials of u and d quarks and the gap, respectively. Note that $\delta\mu$ is just equal to a half of the electron chemical potential μ_e when the vector interaction is absent, and this quantity is to be replaced by an effective chemical potential $\delta\tilde{\mu}$ (see below) when the vector interaction is present, as shown in [30]. The instability of the asymmetric homogenous CSC phase should imply the existence of a yet unknown but stable phase in this region of the T-μ plane. Candidates of such a stable phase include the Larkin-Ovchinnikov-Fulde-Ferrel phase [43] and gluonic phase [44]. Besides developing the possible new phases, the instability problem may also be totally or partially gotten rid of by some other mechanisms. For instance, the instability problem becomes less severe simply at finite temperature because the smeared Fermi surface relaxes the mismatch of the Fermi spheres of the asymmetric quark matter [45–47]. Furthermore, it is known that the larger the quark mass and the stronger the diquark coupling, the more suppressed the instability even at zero temperature [48]. Recently, the present authors [30] have shown that the repulsive vector interaction can also resolve the instability problem totally or partially. The stability by the vector interaction is realized due to the following two ingredients: (1) the density difference between the u and d quarks reduces the mismatch in the effective chemical potentials; (2) the nonzero vector interaction suppresses the formation of high density and hence larger quark masses than those obtained without the interaction are realized. We shall show that the new anomaly term plays a quite similar role as the vector interaction and the interplay between the chiral and diquark condensates induced by the anomaly term acts toward suppressing the unstable region of the homogeneous 2CSC phase in the T-μ plane; the neutral 2CSC phase can become even free from the chromomagnetic instability if K' is larger than a critical value K'_c, which can be reduced significantly when the vector interaction is incorporated.

This paper is organized as follows. In Sec. II, the two-plus-one-flavor NJL model with the extended flavor-mixing six-quark interaction is introduced under the constraints of the charge neutrality and β equilibrium. The phase diagram of the neutral strongly interacting matter with the influence of the axial anomaly is presented in Sec. III. Section IV focuses on the role of the axial anomaly on the chromomagnetic (in)stability. The conclusion and outlook are given in Sec. V.

II. NJL MODEL WITH AXIAL-ANOMALY AND VECTOR INTERACTION

A. The model lagrangian

We start from the following two-plus-one-flavor NJL model with the vector interaction [30,49] and two types of six-quark anomaly terms,

$$\mathcal{L} = \bar{\psi}(i\partial - \hat{m})\psi + \mathcal{L}_\chi^{(4)} + \mathcal{L}_d^{(4)} + \mathcal{L}_\chi^{(6)} + \mathcal{L}_{\chi d}^{(6)}, \quad (1)$$

where $\hat{m} = \mathrm{diag}_f(m_u, m_d, m_s)$ denotes the current-quark mass matrix and

$$\mathcal{L}_\chi^{(4)} = G_S \sum_{i=0}^{8}[(\bar{\psi}\lambda_i^f\psi)^2 + (\bar{\psi}i\gamma_5\lambda_i^f\psi)^2] - G_V \sum_{i=0}^{8}[(\bar{\psi}\gamma^\mu\lambda_i^f\psi)^2 + (\bar{\psi}\gamma^\mu\gamma_5\lambda_i^f\psi)^2], \quad (2)$$

$$\mathcal{L}_d^{(4)} = G_D \sum_{i,j=1}^{3}[(\bar{\psi}i\gamma_5 t_i^f t_j^c \psi_C)(\bar{\psi}_C i\gamma_5 t_i^f t_j^c \psi) + (\bar{\psi}t_i^f t_j^c \psi_C)(\bar{\psi}_C t_i^f t_j^c \psi)], \quad (3)$$

$$\mathcal{L}_\chi^{(6)} = -K\{\det_f[\bar{\psi}(1+\gamma_5)\psi] + \det_f[\bar{\psi}(1-\gamma_5)\psi]\}, \quad (4)$$

$$\mathcal{L}_{\chi d}^{(6)} = \frac{K'}{8}\sum_{i,j,k=1}^{3}\sum_{\pm}[(\psi t_i^f t_k^c(1\pm\gamma_5)\psi_C) \times (\bar{\psi}t_j^f t_k^c(1\pm\gamma_5)\bar{\psi}_C)(\bar{\psi}_i(1\pm\gamma_5)\psi_j)]. \quad (5)$$

Here the four-fermion interactions are all invariant under the $U(3)_R \times U(3)_L$ transformation in the flavor space. In our notations, the Gell-Mann matrices in flavor (color) space are $\lambda_i^{f(c)}$ with $i = 1, \ldots, 8$, and $\lambda_0^{f(c)} \equiv \sqrt{2/3}\mathbb{1}_{f(c)}$, and the antisymmetric one is denoted by $t_i^{f(c)}$ with $i = 1, 2, 3$:

$$t_1^{f(c)} = \lambda_7^{f(c)}, \qquad t_2^{f(c)} = \lambda_5^{f(c)}, \qquad t_3^{f(c)} = \lambda_2^{f(c)}. \quad (6)$$

The scalar interaction in $\mathcal{L}_\chi^{(4)}$ is responsible for the dynamical chiral symmetry breaking in the vacuum with the formation of the chiral condensate, while the vector interaction can be used to investigate the effect of density-density interaction on the chiral phase transition [30].[3] In Eqs. (3) and (5), ψ_C stands for $C\bar{\psi}^T$ and $C = i\gamma_0\gamma_2$ is the Dirac charge conjugation matrix. We remark that the suffix 3 in t_3^f denotes the channel for the u-d pairing, for example. For lower temperature T and large enough baryon chemical

[3]We remark that the effects of the vector interaction on the baryon-number susceptibility and the chiral transition in the two-flavor case are examined in [50] and [16,27], respectively.

potential μ, $\mathcal{L}_d^{(4)}$ leads to the formation of diquark condensate in the color-antitriplet channel [3,41,42]. Besides the four-fermion interactions, Lagrangian (1) also contains two types of six-quark interactions, $\mathcal{L}_\chi^{(6)}$ and $\mathcal{L}_{\chi d}^{(6)}$: the former is the traditional Kobayashi-Maskawa-'tHooft (KMT) interaction [51,52] and its effect on the phase diagram in T-μ plane is fully examined [11,14,18,53–55], whereas the latter could be obtained by a Fierz transformation of the former and induces the coupling between the chiral and diquark condensates [3,34,35,37,39]. We remark that both interactions respect the flavor symmetry of $SU(3)_R \times SU(3)_L \times U(1)$ while violating the $U_A(1)$ symmetry as mentioned above. The former is responsible for accounting for the abnormally large mass of η' beyond the Weinberg inequality [56] (in contrast to other pseudo Nambu-Goldstone bosons) in the effective chiral model and can be identified as an induced quark interaction from instantons [52,57]. The introduction of the latter to the Lagrangian expands the study of CSC to the six-fermion level [35].

B. The model parameters

The numerical values of some model parameters are given in Table I. In contrast to [39], we only consider the case with realistic quark masses. The choice of the model parameters is the same as that in [20,30,40] (all following Ref. [58]), where G_S, the coupling constant for the scalar meson channel, and K, the coupling constant of the KMT term, are fixed by the vacuum physical observables (meson masses and decay constants). We shall work in the isospin symmetric limit in two-flavor space with $m_u = m_d = 5.5$ MeV, and a sharp three-momentum cutoff Λ is adopted.

In contrast to G_S and K, no definite observables in the vacuum are available for determining the coupling constants G_V, G_D, and K' in such a quark model, although we could read off their values from a Fierz transformation of known vertices: the coupling constant K', for instance, can be related to K through the Fierz transformation of the instanton vertex, and K' is found to be identical to K [39]. Since we are mainly interested in the roles of K' and G_V on the chiral phase transition and the chromomagnetic instability, both these coupling constants are treated as free parameters in the present work. Following [39,40], we only consider the attractive interaction between the chiral condensate and the diquark condensate. Namely, the coupling K' is kept positive. As for the ratio of G_D/G_S, we adopt the standard value from Fierz transformation in this paper. Because of the contribution from the KMT interaction, the ratio G_D/G_S from Fierz transformation should be 0.95 rather than 0.75 obtained by only considering the four-quark interaction [14]. Such a choice of the coupling has also been used in Refs. [30,40]. In the literature, the diquark-diquark interaction near the standard value from Fierz transformation is usually called the intermediate coupling.

C. Thermodynamic potential with the constraints of charge-neutrality and β equilibrium

The grand partition function of the NJL model is given by

$$Z \equiv e^{-\Omega V/T} = \int D\bar{\psi} D\psi e^{i \int dx^4 (\mathcal{L} + \psi^\dagger \hat{\mu} \psi)}, \tag{7}$$

where Ω is the thermodynamic potential density and $\hat{\mu}$ is the quark chemical potential matrix. In general, the quark chemical potential matrix $\hat{\mu}$ takes the form [59]

$$\hat{\mu} = \mu - \mu_e Q + \mu_3 T_3 + \mu_8 T_8, \tag{8}$$

where μ is the quark chemical potential (i.e. one third of the baryon chemical potential), μ_e the chemical potential associated with the (negative) electric charge, and μ_3 and μ_8 represent the color chemical potentials corresponding to the Cartan subalgebra in the SU(3)-color space. The explicit form of the electric charge matrix is $Q = \mathrm{diag}(\frac{2}{3}, -\frac{1}{3}, -\frac{1}{3})$ in flavor space, and the color charge matrices are $T_3 = \mathrm{diag}(\frac{1}{2}, -\frac{1}{2}, 0)$ and $T_8 = \mathrm{diag}(\frac{1}{3}, \frac{1}{3}, -\frac{2}{3})$ in the color space. The chemical potentials for the quarks with respective flavor and color charges are listed below:

$$\begin{aligned}
\mu_{ru} &= \mu - \tfrac{2}{3}\mu_e + \tfrac{1}{2}\mu_3 + \tfrac{1}{3}\mu_8, \\
\mu_{rd} &= \mu + \tfrac{1}{3}\mu_e + \tfrac{1}{2}\mu_3 + \tfrac{1}{3}\mu_8, \\
\mu_{rs} &= \mu + \tfrac{1}{3}\mu_e + \tfrac{1}{2}\mu_3 + \tfrac{1}{3}\mu_8, \\
\mu_{gu} &= \mu - \tfrac{2}{3}\mu_e - \tfrac{1}{2}\mu_3 + \tfrac{1}{3}\mu_8, \\
\mu_{gd} &= \mu + \tfrac{1}{3}\mu_e - \tfrac{1}{2}\mu_3 + \tfrac{1}{3}\mu_8, \\
\mu_{gs} &= \mu + \tfrac{1}{3}\mu_e - \tfrac{1}{2}\mu_3 + \tfrac{1}{3}\mu_8, \\
\mu_{bu} &= \mu - \tfrac{2}{3}\mu_e - \tfrac{2}{3}\mu_8, \\
\mu_{bd} &= \mu + \tfrac{1}{3}\mu_e - \tfrac{2}{3}\mu_8, \\
\mu_{bs} &= \mu + \tfrac{1}{3}\mu_e - \tfrac{2}{3}\mu_8.
\end{aligned} \tag{9}$$

TABLE I. The parametrization of two-plus-one-flavor NJL is shown.

$m_{u,d}$ [MeV]	m_s [MeV]	$G_S\Lambda^2$	$K\Lambda^5$	Λ [MeV]	$M_{u,d}$ [MeV]
5.5	140.7	1.835	12.36	602.3	367.7
f_π [MeV]	m_π [MeV]	m_K [MeV]	$m_{\eta'}$ [MeV]	m_η [MeV]	M_s [MeV]
92.4	135	497.7	957.8	514.8	549.5

Corresponding to the chiral and diquark interactions in Eq. (1), we assume that the following condensates are formed in the system, namely, the scalar quark-antiquark condensate:

$$\sigma_i = \langle \bar{\psi}_i \psi_i \rangle, \tag{10}$$

and the scalar diquark condensate

$$s_i = \langle \bar{\psi}_C i\gamma_5 t_i^f t_i^c \psi \rangle. \tag{11}$$

In addition, we remark that the quark-number (or baryon-number) density

$$\rho_i = \langle \bar{\psi}_i \gamma^0 \psi_i \rangle, \tag{12}$$

has a finite value for finite μ. Note that the indices 1, 2, and 3 in Eqs. (10) and (12) represent u, d, and s quarks, respectively, whereas in Eq. (11), the indices 1, 2, and 3 stand for the diquark condensate in d-s, s-u, and u-d pairing channels, respectively. Here we have assumed the condensates and the density are all homogeneous; the study of the phase structure with inhomogeneous condensates and/or baryon-number density [43,60–63] is surely intriguing but beyond the scope of the present work.

The constituent quark masses and the dynamical Majarona masses are expressed in terms of these condensates as follows:

$$M_i = m_i - 4G_S\sigma_i + K|\varepsilon_{ijk}|\sigma_j\sigma_k + \frac{K'}{4}|s_i|^2, \tag{13}$$

and

$$\Delta_i = 2\left(G_D - \frac{K'}{4}\sigma_i\right)s_i. \tag{14}$$

Similarly, it is convenient to define the dynamical quark chemical potential for flavor i by

$$\tilde{\mu}_i = \mu_i - 4G_V\rho_i. \tag{15}$$

A few remarks are in order here:

(1) Both types of the anomaly terms $\mathcal{L}_\chi^{(6)}$ and $\mathcal{L}_{\chi d}^{(6)}$ contribute to the constituent quark masses in Eq. (13), and thus if K' and the diquark condensate s_i are finite, chiral symmetry is dynamically broken even when the usual chiral condensates are absent.

(2) The new anomaly term $\mathcal{L}_{\chi d}^{(6)}$ also modifies the formula for the Majarona mass for the CSC phase so that the chiral condensates affects the Majorana mass, and hence induce an interplay between the two condensates: Indeed the "bare" diquark-diquark coupling G_D is replaced by an effective one, $G'_{Di} \equiv G_D - \frac{K'}{4}\sigma_i$, as shown in Eq. (14), which is dependent on the chiral condensates. Thus the flavor-dependent effective coupling G'_{Di} is now dependent on T and μ through σ_i.

(3) Equations. (13) and (14) clearly show that the flavor-mixing occurs not only in the usual chiral condensates due to $\mathcal{L}_\chi^{(6)}$ but also in the diquark condensates owing to $\mathcal{L}_{\chi d}^{(6)}$, which would lead to interesting physical consequences.

(4) It is also to be noted that the dynamical quark chemical potential $\tilde{\mu}_i$ for u and d quarks are different from each other because of the constraint of electric charge neutrality ($\mu_d > \mu_u$) in 2CSC; notice also, however, that they are dependent only on the respective density $\rho_{u,d}$ and hence the dynamical chemical potentials $\tilde{\mu}_{u,d}$ tend to come closer because $\rho_d > \rho_u$ with the common coupling constant G_V [30].

In the mean-field level, the thermodynamic potential for the two-plus-one-flavor NJL with the charge-neutrality constraints reads

$$\Omega = \Omega_l + 2G_S\sum_{i=1}^{3}\sigma_i^2 - 2G_V\sum_{i=1}^{3}\rho_i^2 + \sum_{i=1}^{3}\left(G_D - \frac{K'}{2}\sigma_i\right)|s_i|^2 - 4K\sigma_1\sigma_2\sigma_3 - \frac{T}{2V}\sum_P \ln\det\frac{S_{MF}^{-1}}{T}. \tag{16}$$

Notice the presence of the new cubic-mixing terms among the chiral and diquark condensates. In Eq. (16), Ω_l denotes the contribution from free leptons. Note that Ω_l should include the contributions from both electrons and muons for completeness. Since $M_\mu \gg M_e$ and $M_e \approx 0$, ignoring the contribution of muons has little effect on the phase structure. Therefore, only electrons are considered in our calculation and the corresponding Ω_l reads

$$\Omega_l = -\frac{1}{12\pi^2}\left(\mu_e^4 + 2\pi^2T^2\mu_e^2 + \frac{7\pi^4}{15}T^4\right). \tag{17}$$

Because of the large mass difference between s and $u\,[d]$ quarks, the most favored phase at low temperature and moderate density tends to be the 2CSC rather than CFL phase, as demonstrated in the two-plus-one-flavor NJL model [20,21]. Surprisingly enough, if the anomaly term $\mathcal{L}_{\chi d}^{(6)}$ is incorporated, the 2CSC phase turns to be still favored in the intermediate density region even when the three flavors have the equal mass [40]. Needless to say, the dominance of the 2CSC phase over the CFL one is more robust when the realistic mass hierarchy for the three flavors is adopted. Moreover, it is worth mentioning here that the mass disparity favors the 2CSC phase with the u-d pairing also through the inequality of the effective diquark coupling $G'_{D3} > G'_{D1,2}$ when the anomaly coupling K' is present; see Eq. (14). Since the main purpose of the present work is to explore how the axial-anomaly term $\mathcal{L}_{\chi d}^{(6)}$

affects the phase boundary involving the chiral transition at moderate densities, under the constraints of the charge neutrality and β equilibrium, we only consider the 2CSC phase in the following. Note that μ_3 in (8) vanishes in the 2CSC phase because the color SU(2) symmetry for the red and green quarks are left unbroken.

The inverse quark-propagator matrix in the Nambu-Gorkov formalism takes the following form in the mean-field approximation:

$$S_{\mathrm{MF}}^{-1}(i\omega_n, \vec{p}) = \begin{pmatrix} [G_0^+]^{-1} & \Delta\gamma_5 t_3^f t_3^c \\ -\Delta^* \gamma_5 t_3^f t_3^c & [G_0^-]^{-1} \end{pmatrix}, \tag{18}$$

with

$$[G_0^{\pm}]^{-1} = \gamma_0(i\omega_n \pm \hat{\tilde{\mu}}) - \vec{\gamma}\cdot\vec{p} - \hat{M}, \tag{19}$$

where $\hat{M} = \mathrm{diag}_f(M_u, M_d, M_s)$, $\hat{\tilde{\mu}} = \mathrm{diag}_f(\tilde{\mu}_u, \tilde{\mu}_d, \tilde{\mu}_s)$, and $\omega_n = (2n+1)\pi T$ is the Matsubara frequency. Taking the Matsubara sum, the last part of the thermodynamic potential (16) is expressed as

$$-\frac{T}{2V}\sum_P \ln\det\frac{S_{MF}^{-1}}{T} = -\sum_{i=1}^{18}\int\frac{d^3p}{(2\pi)^3}\{(E_i - E_i^0) + 2T\ln(1+e^{-E_i/T})\}, \tag{20}$$

with the dispersion relations for nine quasiparticles [that is, three flavors $\times$ three colors; the spin degeneracy is already taken into account in Eq. (20)] and nine quasi-antiparticles. In Eq. (20), E_i^0 represents $E_i(M = m, \Delta = 0, \rho = 0)$. The s quark and unpaired blue u and d quarks have 12 energy dispersion relations with a similar form. For example, the dispersion relations for the blue u quark and anti-blue u quark are

$$E_{bu} = E - \tilde{\mu}_{bu} \quad \text{and} \quad \bar{E}_{bu} = E + \tilde{\mu}_{bu}, \tag{21}$$

respectively, with $E = \sqrt{\vec{p}^2 + M_u^2}$. In the rd-gu quark sector with pairing we can find the four dispersion relations,

$$\begin{aligned} E^{\pm}_{rd\text{-}gu} &= E_\Delta \pm \tfrac{1}{2}(\tilde{\mu}_{rd} - \tilde{\mu}_{gu}) = E_\Delta \pm \delta\tilde{\mu}, \\ \bar{E}^{\pm}_{rd\text{-}gu} &= \bar{E}_\Delta \pm \tfrac{1}{2}(\tilde{\mu}_{rd} - \tilde{\mu}_{gu}) = \bar{E}_\Delta \pm \delta\tilde{\mu}, \end{aligned} \tag{22}$$

and the ru-gd sector has another four as

$$\begin{aligned} E^{\pm}_{rd\text{-}gu} &= E_\Delta \pm \tfrac{1}{2}(\tilde{\mu}_{ru} - \tilde{\mu}_{gd}) = E_\Delta \mp \delta\tilde{\mu}, \\ \bar{E}^{\pm}_{rd\text{-}gu} &= \bar{E}_\Delta \pm \tfrac{1}{2}(\tilde{\mu}_{ru} - \tilde{\mu}_{gd}) = \bar{E}_\Delta \mp \delta\tilde{\mu}, \end{aligned} \tag{23}$$

where $E_\Delta = \sqrt{(E - \bar{\tilde{\mu}})^2 + \Delta^2}$ and $\bar{E}_\Delta = \sqrt{(E + \bar{\tilde{\mu}})^2 + \Delta^2}$; from now on Δ stands for Δ_3. The average chemical potential is defined by

$$\bar{\tilde{\mu}} = \frac{\tilde{\mu}_{rd} + \tilde{\mu}_{gu}}{2} = \frac{\tilde{\mu}_{ru} + \tilde{\mu}_{gd}}{2} = \mu - \frac{\mu_e}{6} - 2G_V(\rho_1 + \rho_2) + \frac{\mu_8}{3}, \tag{24}$$

and the effective mismatch between the chemical potentials of u and d quarks takes the form

$$\delta\tilde{\mu} = \tfrac{1}{2}(\mu_e - 4G_V(\rho_2 - \rho_1)). \tag{25}$$

Ignoring the mass difference between u and d quarks, the determinantal term in Eq. (16) has an analytical form which greatly simplifies the numerical calculation. Adopting the variational method, we get the eight nonlinear coupling equations

$$\frac{\partial\Omega}{\partial\sigma_1} = \frac{\partial\Omega}{\partial\sigma_3} = \frac{\partial\Omega}{\partial s_3} = \frac{\partial\Omega}{\partial\rho_1} = \frac{\partial\Omega}{\partial\rho_2} = \frac{\partial\Omega}{\partial\rho_3} = \frac{\partial\Omega}{\partial\mu_e} = \frac{\partial\Omega}{\partial\mu_8} = 0. \tag{26}$$

Since μ_8 is tiny around the chiral transition region [20,21], we shall set it zero with little effect in the numerical results [30]. Thus, Eq. (26) is then simplified to a system of seven coupled equations.

III. PHASE STRUCTURE WITH THE AXIAL ANOMALY

In this section, we show numerical results of the effects of the new six-quark interaction (5) on the chiral phase transition under the charge-neutrality and β-equilibrium constraints with or without the vector interaction. Since we are mainly interested in the phase diagram involving chiral transition at low temperatures, all the phase diagrams will be plotted for the range 250 MeV $< \mu <$ 400 MeV where the chiral transition is expected to be relevant. As for the type of the CSC phase, Ref. [40] indicates that the CFL phase is only realized for $\mu > 460$ MeV even when $K' = 0$ with the same model parameters as ours, and an increase of K' pushes the CFL phase to even higher μ region. Therefore, we exclusively consider the 2CSC phase near the chiral boundary without a loss of generality.

In the following, we use the same notations as in Refs. [29,30,36] to distinguish the different regions in the T-μ phase diagram. Namely, NG, CSC, COE, and NOR refer to the hadronic (Nambu-Goldstone) phase with $\sigma \neq 0$ and $\Delta = 0$, color-superconducting phase with $\Delta \neq 0$ and $\sigma = 0$, coexisting phase with $\sigma \neq 0$ and $\Delta \neq 0$, and normal phase with $\sigma = \Delta = 0$, respectively, though they have exact meanings only in the chiral limit.

A. The case without vector interaction

We first show the numerical results in the case without the vector interaction. The phase diagrams with varying coupling constant K' are displayed in Fig. 1. In contrast to Fig. 8 in Ref. [40], the multi-CP structure can still appear with a choice of K' in the phase diagram when the charge neutrality, β equilibrium, and the new axial-anomaly term are simultaneously taken into account. For $K'/K = 2.0$, Fig. 1(a) shows that there exists only one usual chiral CP even though the COE emerges: We remark that the COE

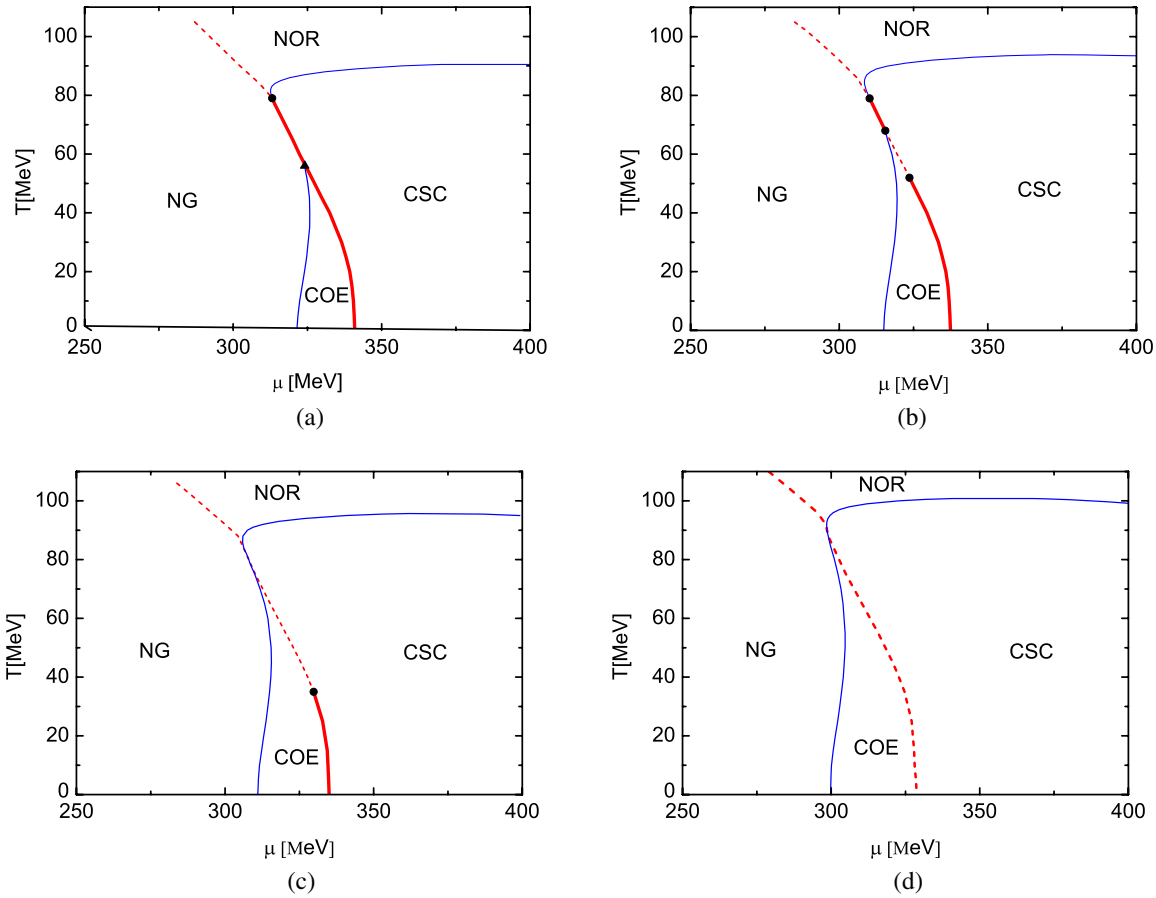

FIG. 1 (color online). The phase diagrams in the T-μ plane for various values of K' in the two-plus-one-flavor NJL model with the charge-neutrality and β-equilibrium being kept. The vector interaction is not taken into account. The thick solid line, thin solid line, and dashed line denote the first-order transition, second-order transition, and chiral crossover, respectively. (a) $K'/K = 2.0$, (b) $K'/K = 2.25$, (c) $K'/K = 2.4$, and (d) $K'/K = 2.8$

region does not exist when $K'/K = 0$, which is not displayed in Fig. 1. Figure 1(b) shows that when K'/K is increased to 2.25, the chiral transition turns to a crossover at relatively lower temperatures, and hence there appear two new chiral CPs. With a further increase of K'/K, the boundary line for first-order transition at higher temperature shrinks and thus the two crossover boundary lines in Fig. 1(b) join with each other, and eventually only one CP is left in the phase diagram, as shown in Fig. 1(c). When K'/K is large enough, Fig. 1(d) indicates that the first-order boundary vanishes completely and there is no chiral CP in the phase diagram.

We note that the emergence of the three CPs in Fig. 1(b) comes from a joint effect of the interplay between the chiral and diquark condensates and the electric charge-neutrality constraint. First of all, we recall that the abnormal thermal behavior of the diquark condensate that it has a maximum at a finite temperature in the COE is responsible for the emergence of the multiple chiral CP structure [27–30]. Such a behavior is also observed in the present case, as displayed in Fig. 1(b). As first indicated in Ref. [29], when $\mu_e = \mu_d - \mu_u$ is positive, the boundary of the chiral transition is shifted toward the higher μ region, and leads to the formation of the COE at the low-temperature region, in which the chiral phase transition is significantly weakened by the smearing of the Fermi surface inherent in the CSC phase. In this regard, μ_e plays a role of an effective vector interaction [27,28,30]. On the other hand, the chiral anomaly term with positive K' intensifies the competition between the chiral and diquark condensates due to the enhanced effective diquark-diquark interaction. Thus, when K' is increased, the CSC region expands toward the lower μ region in the T-μ plane. Consequently, the COE region tends to be more easily formed when both μ_e and K' take effect. Therefore, the chiral transition is significantly weakened and the smooth crossover gets to appear with new CPs in the intermediate temperature owing to the abnormal thermal behavior of the diquark condensate.

The T dependence of M_u, M_s, Δ, and $\delta\tilde{\mu}$ for fixed $K'/K = 2.25$ and several values of μ is shown in Fig. 2. One can see that, with increasing T, the constituent quark masses decrease persistently while the Majarona mass for CSC first increases, has the maximum value, and then

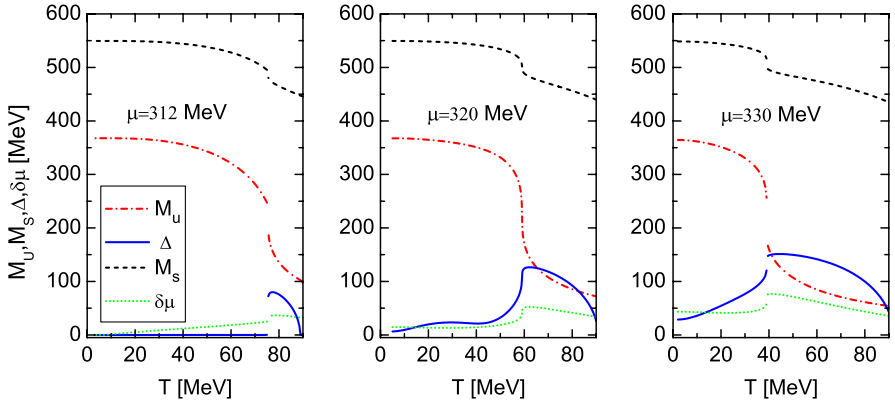

FIG. 2 (color online). The temperature dependence of M_u, M_s, Δ, and $\delta\tilde{\mu}$ for fixed $K'/K = 2.25$ and three different chemical potentials $\mu = 312$ MeV, 320 MeV, and 330 MeV. The constraints of electric charge neutrality and β equilibrium are imposed while the vector interaction is not incorporated.

decreases in the COE region and nearby. Let us see the details for each value of μ. For a small $\mu = 312$ MeV, the diquark pairing is weak and the gap Δ does not appear at the lower-temperature region. Thus, the chiral phase transition keeps the nature of the first order at $T_{C1} \approx 75$ MeV. At a lager $\mu = 320$ MeV, the diquark pairing becomes significant and the Δ shows the abnormal thermal behavior with a maximum value around $T_{C2} \approx 60$ MeV, and hence the chiral phase transition turns to a smooth crossover owing to the competition with the diquark condensate in the COE region. For even larger $\mu = 330$ MeV, the diquark pairing becomes more significant and the Δ still shows the abnormal thermal behavior. However, the competition between the two condensates is not strong enough to qualitatively change the nature of the chiral restoration and a first-order transition happens at $T_{C3} \approx 40$ MeV. The reason why the crossover does not occur at $\mu = 330$ MeV but happens at $\mu = 320$ MeV can be understood as follows: Starting from the same point ($T = T_{C3}$, $\mu = 320$ MeV) in the COE region, an increase of T affects the nature of the chiral transition more significantly than that of μ does, since $T_{C3} < T_{C2}$.

We have seen that the abnormal thermal behavior of the gap Δ plays an essential role in realizing the multi-CP structure of the phase diagram. Such an unusual T dependence of the Δ can be attributed to the following two mechanisms: (i) the mismatch between the chemical potentials of u and d quarks owing to the charge-neutrality and β-equilibrium constraints and (ii) the small Fermi spheres of the quarks in the COE region due to the relatively large quark masses: First, the difference in the chemical potentials $\delta\tilde{\mu}$ or the mismatch of the Fermi momenta disfavors the u-d pairing at zero or small temperature. However, as the temperature is raised in the low-T region, more and more u and d quarks tend to participate in the pairing due to the smearing of the Fermi surfaces, especially that of the u quark. Of course, when T is raised too much, the pairing will be gradually destroyed. Thus, the Δ will have the maximum value at a finite T and then disappear eventually when T is further raised. These dual effects of the temperature on the diquark pairing lead to the abnormal behavior of the Δ. This behavior becomes more prominent in the 2CSC phase for a weak diquark coupling [64] or in the COE region for a moderate or strong diquark coupling [29,30]. Second, when T is raised, the dynamical quark masses decrease and hence the Fermi spheres or momenta of u and d quarks grow significantly for a fixed μ, which means that the density of states at the Fermi surface increases with T, and thus the diquark pairing is enhanced in the COE region. The increased diquark condensates in turn tend to further suppress the dynamical quark masses.

Notice that such an increase of the diquark condensate along with increasing T is expected to be most prominent around the phase boundary of the chiral transition, including the COE region, where the chiral condensates change most significantly. For the neutral 2CSC, once the COE is formed, both of these mechanisms take effects simultaneously and are mutually enhanced, and thus the formation of the multiple-CP structure is readily made.

This may explain why no intermediate-temperature CP is realized in Ref. [40] where the chiral-diquark interplay is embodied by the anomaly term but without the charge-neutrality and β-equilibrium constraints; the anomaly term solely is insufficient for realizing the abnormal thermal behavior of the Δ. It should be stressed that the mechanism for the emergence of the intermediate-temperature CPs in Fig. 1(b) is apparently similar to that in the two-flavor case found in [29]. However, the strange quark plays an important role in the present case since the chiral condensate of the strange quark contributes positively to the effective diquark-diquark coupling for u and d quarks through the axial anomaly. We should stress that apart from the appearance of intermediate-temperature CPs, there is a common feature with and without the charge-neutrality constraint: the chiral transition in the low-T region extending zero temperature keeps first order provided that K' does not

exceed a critical value at which the first-order line completely disappears.

Last but not least, we remark that the T-μ region where the two new low-temperature CPs are located in Fig. 1(b) is free from the chromomagnetic instability, which is obvious from Fig. 5(a); a detailed discussion on this point will be given in Sec. IV.

B. The case for nonzero vector interaction

In this subsection, we will investigate the phase diagram when both the vector and the new six-quark interactions are present under the charge-neutrality and β-equilibrium constraints.

There are some choices for the value of the vector coupling: The chiral instanton-anti-instanton molecule model [57] gives the ratio $G_V/G_S = 0.25$, while the Fierz transformation of the vertex given in the truncated Dyson-Schwinger model [65] gives the ratio 0.5. Thus, we rather treat the G_V/G_S as a free parameter in the range, 0–0.5.

We first explore the phase diagram in the T-μ plane by varying the ratio K'/K but with G_V/G_S being fixed as 0.25, the value given in the instanton-anti-instanton molecule model. When K'/K is small and less than 0.5, only the usual phase structure with single CP is obtained. When K'/K exceeds 0.5, four different types of the CP structures appear, as displayed in Fig. 3. At $K'/K = 0.55$, a phase diagram similar to that in Fig. 1(b) is obtained, as shown in Fig. 3(a), where two new intermediate-temperature CPs emerge. When K'/K is slightly increased to 0.57, the chiral transition becomes crossover in the lower-temperature region which extends to zero temperature; thus the total number of the CPs becomes four, which indicates stronger competition between the chiral and diquark condensates at relatively larger μ. Further increasing K'/K, the low-temperature chiral boundary totally turns into a crossover one and only one first-order transition line with two CPs attached remains in the phase diagram, as displayed in Fig. 3(c). In this case, the number of the CPs is reduced to two accordingly. When K'/K is large enough,

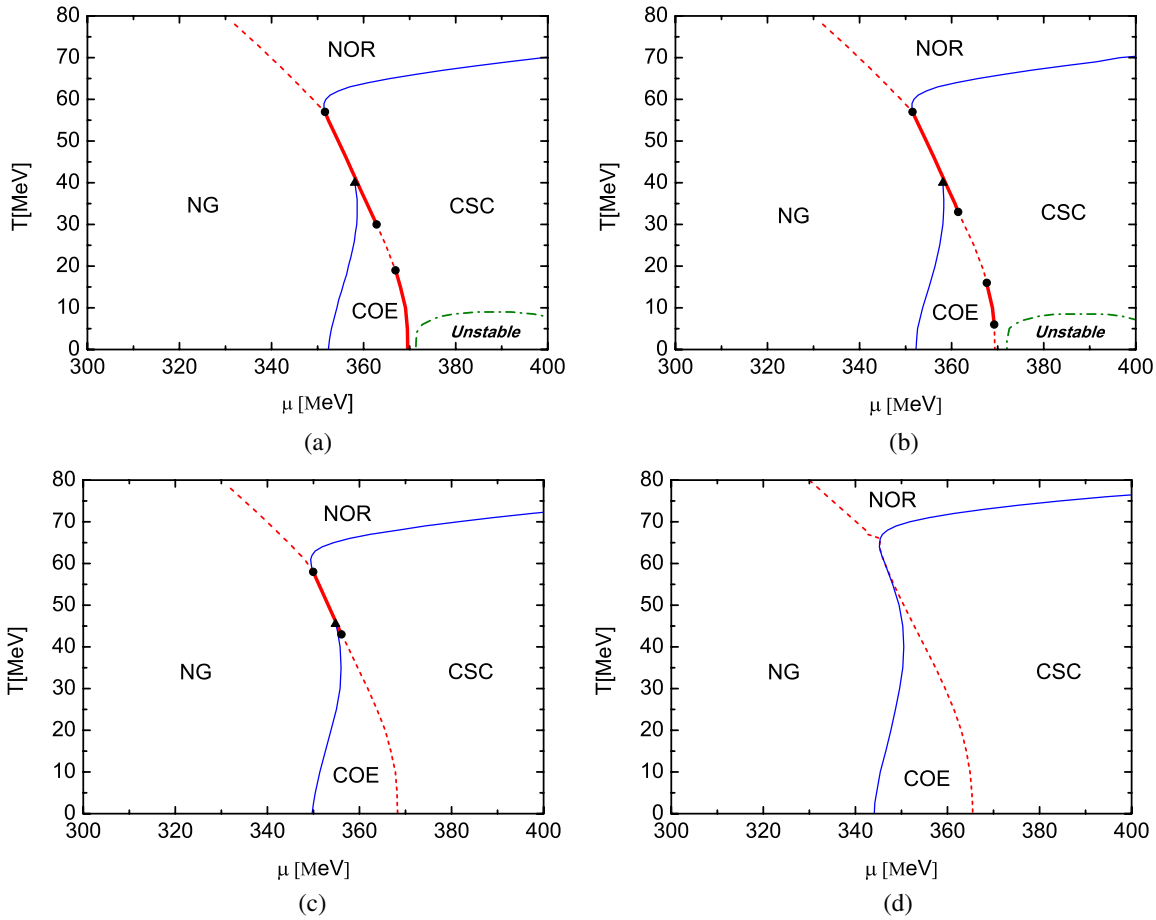

FIG. 3 (color online). The T-μ phase diagrams of the two-plus-one-flavor NJL model for several values of K'/K and fixed $G_V/G_S = 0.25$, where the charge-neutrality constraint and β-equilibrium condition are imposed. With the increase of K'/K, the number of the critical points changes and the unstable region characterized by the chromomagnetic instability (bordered by the dash-dotted line) tends to shrink and ultimately vanishes in the phase diagram. The respective meanings of the various types of lines are the same as those in Fig. 1. (a) $K'/K = 0.55$, (b) $K'/K = 0.57$, (c) $K'/K = 0.70$, and (d) $K'/K = 1.0$

Fig. 3(d) shows that only chiral crossover transition exists in the phase diagram with no CP.

In comparison with Fig. 1 where the vector interaction is not included, Fig. 3 indicates that the phase structures with multiple CPs can be realized with relatively small K' owing to the vector interaction. We remark that all the types of the chiral CP structures displayed in Fig. 3 by varying K' are obtained by varying G_V without the anomaly term [30]. In the present case, the number of the critical points changes as $1 \to 3 \to 4 \to 2 \to$ when K' is increased.

As is mentioned before, the Fierz transformation of the instanton vertex leads to the identity $K' = K$, so it is

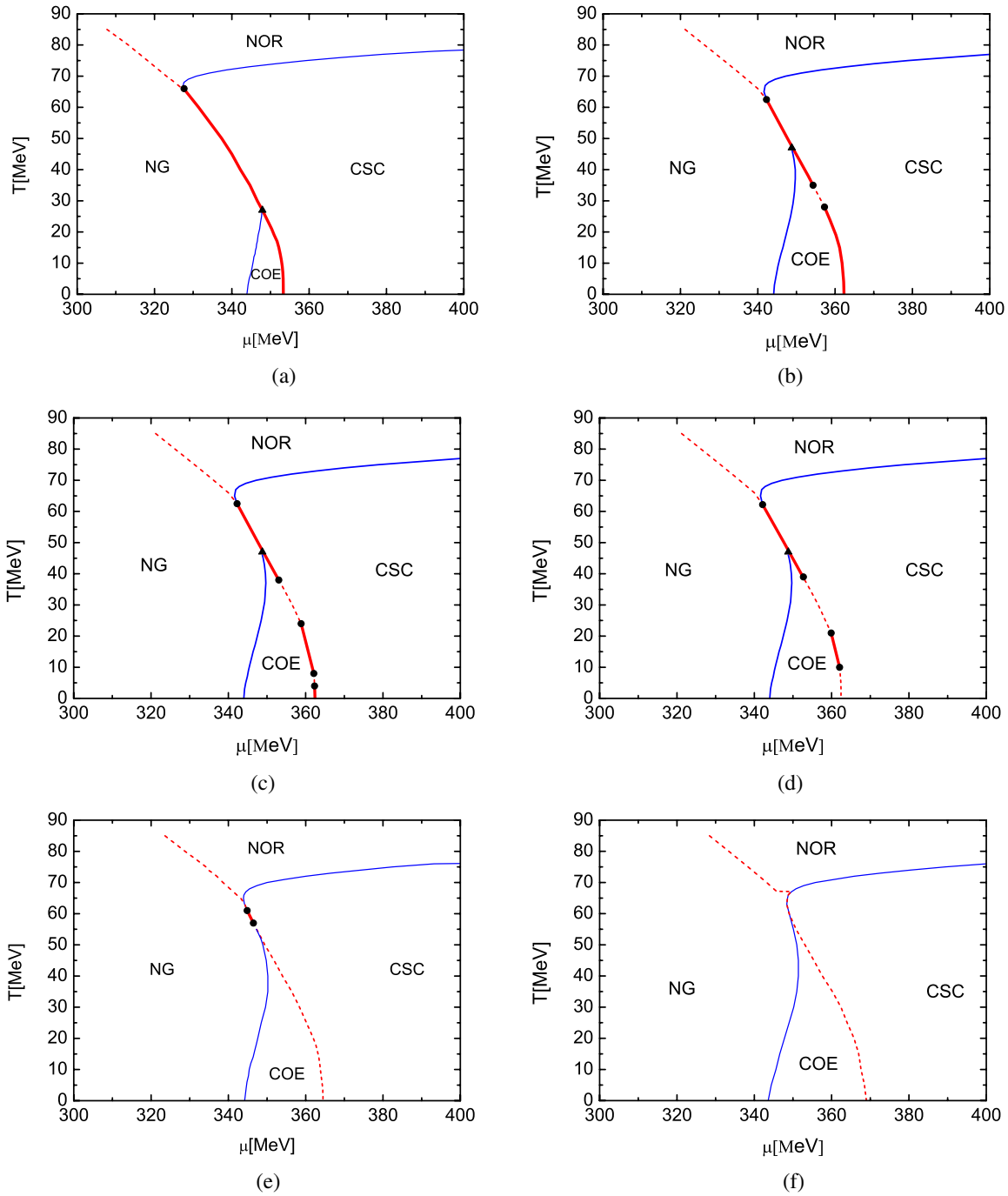

FIG. 4 (color online). The phase diagrams in the two-plus-one-flavor NJL model for fixed $K'/K = 1.0$ with G_V/G_S being varied, where the charge-neutrality constraint and β-equilibrium condition are taken into account. The meanings of the different line types are the same as those in Fig. 1. The number of the critical points changes along with an increase of G_V/G_S. All the phase diagrams are free from the chromomagnetic instability. (a) $G_V/G_S = 0$, (b) $G_V/G_S = 0.193$, (c) $G_V/G_S = 0.195$, (d) $G_V/G_S = 0.197$, (e) $G_V/G_S = 0.23$, and (f) $G_V/G_S = 0.3$

of special interest to investigate the phase diagram in the case of $K' = K$. A series of phase diagrams with fixed $K'/K = 1$ but varied G_V is shown in Fig. 3. One finds that all the chiral CP structures in Fig. 3 still appear in the phase diagrams, and moreover, even as large as five CPs can exist in the phase diagram, as shown in Fig. 4(c). This suggests that the interplay between the chiral and the diquark condensates in the COE region becomes complicated once the charge neutrality, the vector interaction, and the axial anomaly are all taken into account. A comparison with the case of vanishing K', which is given in Fig. 7 in [30], shows that the parameter range of G_V for realizing the low-temperature CPs moves towards lower G_V, which is actually natural because K' gives the same effect as G_V on the chiral transition. It is noteworthy that such lower values of G_V are also close to the standard value of G_V/G_S derived from the instanton model. The number of the CPs changes as $1 \rightarrow 3 \rightarrow 5 \rightarrow 4 \rightarrow 2 \rightarrow$ with increasing G_V.

The anomaly terms in Eq. (1) are supposed to originate from the instantons, which are to be screened at finite chemical potential and temperature [57]. Accordingly, both the coupling constants K and K' are expected to diminish around the phase boundary. However, we emphasize that the main effect of K' is to enhance the chiral condensate of the strange quark and the u-d diquark condensate by each other through the cubic coupling among them for the realistic quark masses, and Figs. 3 and 4 tell us that even smaller values of K' expected at low temperature and moderate density can still lead to a quite different phase structure with multiple CPs when the vector interaction is present under the charge-neutrality constraint.

IV. THE INFLUENCE ON THE CHROMOMAGNETIC INSTABILITY

In this section, we investigate the effect of the new axial-anomaly term on the chromomagnetic instability of the asymmetric homogeneous 2CSC phase by varying K'. We shall show that the anomaly-induced interplay between the chiral and diquark condensates acts toward suppressing the unstable region of the homogeneous 2CSC phase in the T-μ plane. Thus, the 2CSC phase can become even free from the chromomagnetic instability provided that K' is larger than a critical value K'_c, which can be reduced significantly when the vector interaction is incorporated.

The magnetic instability region in the T-μ plane is determined by calculating the Meissner masses squared which can be negative when the charge-neutrality constraint is imposed. Here we adopt the same method as that in [45] to evaluate the Meissner mass squared

$$m_M^2 = \frac{\partial^2}{\partial B^2}[\Omega(\Delta) - \Omega(\Delta = 0)]_{B=0}, \tag{27}$$

where B has the same meaning as that in [45]. Since the strange quark does not take part in the diquark pairing in the present case, we can directly use the formula for the two-flavor NJL model to calculate the Meissner mass squared.

The effect of the coupling constant K' on the chromomagnetic instability is shown in Fig. 5. We have adopted the model parameters in Table I to calculate the Meissner mass squared. Figure 5(a) displays the change of the unstable region of the chromomagnetic instability with varying K' when the vector interaction is not included. One can see that the instability region tends to shrink with increasing K' and eventually vanishes for $K'/K > 0.8$. This suggests that the neutral homogenous 2CSC phase will be totally free from the chromomagnetic instability if $K' = K$ that is derived by the Fierz transformation from the usual instanton vertex. When taking the vector interaction with $G_V/G_S = 0.5$, the unstable region shrinks more significantly with increasing K' and eventually disappears in the T-μ plane for $K'/K > 0.55$, as shown in Fig. 5(b). This

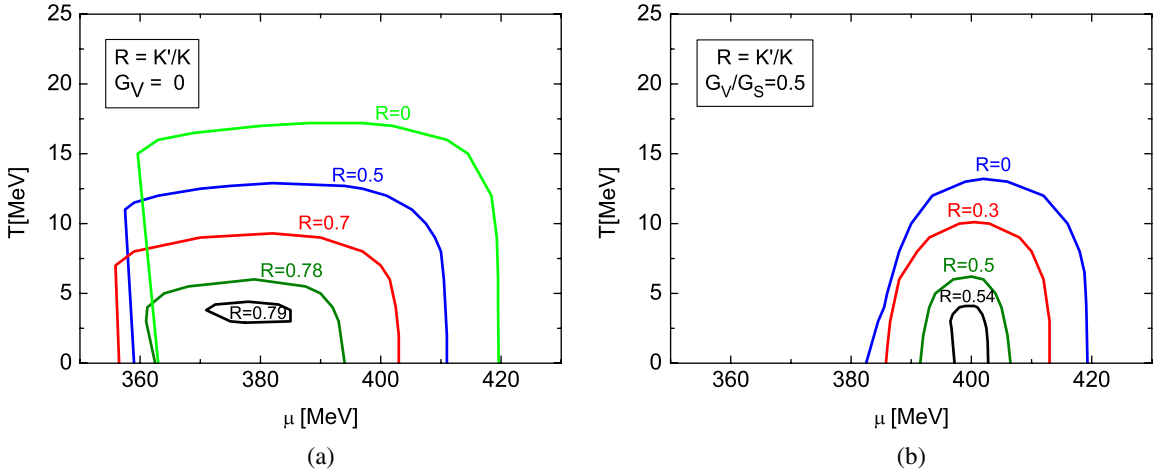

FIG. 5 (color online). The boundary between the stable and unstable homogenous 2CSC regions with (right figure) and without (left figure) the vector interaction in two-plus-one-flavor NJL model. With the increase of the ratio $K'/K \equiv R$, the unstable region with the chromomagnetic instability in the T-μ plane shrinks and eventually vanishes.

could be an expected result because of the effect of the vector interaction on the instability problem found in [30].

The reason for the suppression of the chromomagnetic instability by K' is understood as follows. First of all, Eq. (16) tells us that the u-d diquark coupling is enhanced by the presence of the s quark chiral condensate due to the coupling between the chiral and diquark condensates induced by the K' term. On the other hand, as was first shown in [48] through changing the diquark coupling by hand, the chromomagnetic instability tends to be suppressed in the strong coupling region and can be completely gotten rid of when the diquark coupling is strong enough. Thus we see that the coupling between the u-d diquark and the chiral s-quark condensates by the K' term leads to the suppression of the chromomagnetic instability. This is a new mechanism of the stabilization of the gapless 2CSC phase, found in the present work. We here emphasize the important role of the strange quark and the anomaly term in suppressing the instability: In contrast to the pure two-flavor case, the rather large chiral condensate of the strange quark enhances the diquark coupling between the u and d quarks owing to the axial anomaly in the two-plus-one flavor case, and this enhancement of the diquark coupling causes the stabilization.

Because of their common effects on the chromomagnetic (in)stability, Fig. 5 suggests that the instability may be totally cured in the asymmetric homogeneous 2CSC phase when the coupling constants of the vector interaction and the extended six-quark interaction are in an appropriate range. Admittedly, the present work has only dealt with the case of the so called intermediate diquark coupling. Nevertheless, for a weaker diquark coupling, it is expected that the system can be still free from the chromomagnetic instability only with larger couplings for both the vector interaction and the anomaly K'-term.

V. CONCLUSIONS AND OUTLOOK

We have explored the phase structure and the chromomagnetic instability of the strongly interacting matter under the charge-neutrality constraint within a two-plus-one-flavor NJL model by incorporating a new anomaly term as well as the conventional KMT interaction. The anomaly terms have the forms of six-quark interactions and violate the $U_A(1)$ symmetry as a reflection of the axial anomaly of QCD. Similarly to the KMT term, the new anomaly interaction with the coupling constant K' also induces a flavor mixing which leads to a direct coupling between the chiral and diquark condensates.

We first investigated the role of the axial anomaly on the emergence of the low or intermediate-temperature CP(s) without the vector interaction. Owing to the large strange quark mass, the favored CSC phase near the chiral boundary is 2CSC rather than CFL, where the electric chemical potential μ_e required by the charge-neutrality plays an important role on the chiral phase transition [29]. The once-declared low-temperature CP in the symmetric three-flavor limit [39] was ruled out in Ref. [40] due to the actual dominance of the 2CSC over the CFL. We have shown that this is true under the charge-neutrality constraint without the vector interaction; the chiral transition in the low-T region extending zero temperature keeps first order provided that K' does not exceed a critical value at which the first-order line completely disappears. However, the new chiral anomaly term enhances the competition between the chiral and diquark condensates under the charge-neutrality constraint, and gives rise to the intermediate-temperature CPs for an appropriate range of K'. No such intermediate-temperature CPs had been found in the same model when only either the charge-neutrality constraint or the axial anomaly is exclusively included, as shown in [20,40]; both of which did not take into account the vector interaction, either.

We then investigated the T-μ phase diagram by incorporating the repulsive vector interaction as well: We remark that this task may be viewed as an extension of the work [30], in which the effect of the vector interaction on the phase diagram is fully explored under the charge-neutrality constraint, to incorporate the anomaly term. We have found that the cubic coupling between the chiral and diquark condensates induced by the axial anomaly does not affect the qualitative results obtained in [30]. Rather, the vector interaction and the anomaly term jointly act so that the multiple CPs are realized. Indeed, by varying K' with fixed vector coupling or vise verse, we have shown that all the types of multiple-CP structures obtained in [30] can be reproduced. In particular, the phase transition in the low-T region extending zero temperature becomes a crossover only when the vector interaction is present with a strength larger than a critical value. Furthermore, the maximum number of the CPs can reach as large as five when both the interactions are put on. In this case, the low- and intermediate-temperature CPs can appear even with small values of K' owing to the help by the vector interaction. This is very welcome because K' in the realistic situation at moderate and high density should be weaker than that in the vacuum, since the anomaly term is supposed to originate from the instanton configuration which is expected to be suppressed at finite density.

Besides the influence on the chiral phase transition, we have shown that the axial anomaly also plays an important role on the suppression of the chromomagnetic instability for the asymmetric homogenous 2CSC phase, which is first disclosed in the present work: With an increase of the extended six-quark interaction, the T-μ region with the chromomagnetic instability shrinks and eventually vanishes when the coupling K' is sufficiently large. In particular, when taking into account the vector interaction simultaneously, the chromomagnetic instability is suppressed more significantly and can be completely gotten rid of by the axial anomaly.

A general and remarkable message obtained from the present investigation is that the strange quark can significantly affect the properties of the neutral strongly interacting matter in which the 2CSC phase with u-d pairing is realized: Even though the strange quark does not directly participate in the Cooper pairing in the 2CSC, the interplay between the u-d diquark condensate and the strange chiral condensate induced by the anomaly term can lead to a drastically different phase structure in the T-μ plane under the charge-neutrality constraint.

It should be remarked here that the contribution of other possible cubic flavor-mixing terms composed of different condensates, such as

$$\sigma\rho^2 = \epsilon^{ijk}\sigma_i\rho_j\rho_k, \tag{28}$$

which arise from another type of six-quark interaction

$$\mathcal{L}^{(6)}_{\chi\rho} \sim \epsilon^{ijk}\epsilon^{lmn}(\bar{\psi}_i\gamma^\mu(1\pm\gamma_5)\psi_l)(\bar{\psi}_j\gamma_\mu(1\pm\gamma_5)\psi_m) \times(\bar{\psi}_k(1\pm\gamma_5)\psi_n), \tag{29}$$

are all neglected in Eq. (16) for simplicity. The interaction (29) can be derived from the KMT interaction, which may or may not affect the phase structure. Besides their direct contribution to the thermodynamic potential, these flavor-mixing terms also modify the dispersion relations of the quasiquarks: For example, the dynamical quark mass becomes dependent on the quark-number density through the term $\sigma\rho^2$. It is certainly an interesting problem to explore the possible effects of these cubic coupling terms on the phase diagram; we leave such a task to a future work.

Even apart from the neglect of the above vertex (29), there are some caveats with the present study based on a chiral model that does not embody the confinement effect, and relies on the mean-field approximation. The results obtained in the current study are largely parameter dependent and bears the shortcomings inherent in the mean-field approximation. For instance, the result that there can be multiple CPs associated with the chiral transition and the CSC actually may merely mean that the QCD matter is very soft for a simultaneous formation of the diquark and chiral condensates coupled with the baryonic density along the phase boundary. Of course, a study which incorporates these fluctuations should be performed, say, by means of the nonperturbative/functional renormalization group method [66,67] with the present model used as a bare model. More profoundly, the effect of the confinement should be incorporated even in an effective model approach, which is a more challenging problem since the mechanism of confinement is still unclear. Anyway, further studies based on different models and/or methods are needed to determine whether the low-temperature CP(s) exists. One of the tasks of the future is exploring whether the low-temperature CP(s) persists or not when the inhomogeneous phases are taken into consideration such as the chiral crystalline phase [60–63] or the Larkin-Ovchinnikov-Fulde-Ferrel phase [43].

ACKNOWLEDGMENTS

Z. Z. was supported by the Fundamental Research Funds for the Central Universities of China. T. K. was partially supported by a Grant-in-Aid for Scientific Research by the Ministry of Education, Culture, Sports, Science, and Technology (MEXT) of Japan (No. 20540265), by the Yukawa International Program for Quark-Hadron Sciences, and by the Grant-in-Aid for the global COE program " The Next Generation of Physics, Spun from Universality and Emergence " from MEXT.

[1] M. Cheng *et al.*, Phys. Rev. D **81**, 054510 (2010).
[2] S. Borsanyi, Z. Fodor, C. Hoelbling, S. D. Katz, S. Krieg, C. Ratti, and K. K. Szabo, J. High Energy Phys. 09 (2010) 073; G. Endrodi, Z. Fodor, S. D. Katz, and K. K. Szabo, J. High Energy Phys. 04 (2011) 001.
[3] M. G. Alford, K. Rajagopal, and F. Wilczek, Nucl. Phys. **B537**, 443 (1999).
[4] D. T. Son, Phys. Rev. D **59**, 094019 (1999).
[5] T. Schäfer and F. Wilczek, Phys. Rev. D **60**, 114033 (1999).
[6] I. A. Shovkovy and L. C. R. Wijewardhana, Phys. Lett. B **470**, 189 (1999).
[7] T. Schäfer, Nucl. Phys. **B575**, 269 (2000).
[8] Y. Nambu and G. Jona-Lasinio, Phys. Rev. **122**, 345 (1961); **124**, 246 (1961).
[9] U. Vogl and W. Weise, Prog. Part. Nucl. Phys. **27**, 195 (1991).
[10] S. P. Klevansky, Rev. Mod. Phys. **64**, 649 (1992).
[11] T. Hatsuda and T. Kunihiro, Phys. Rep. **247**, 221 (1994).
[12] K. Rajagopal and F. Wilczek, arXiv:hep-ph/0011333.
[13] D. H. Rischke, Prog. Part. Nucl. Phys. **52**, 197 (2004).
[14] M. Buballa, Phys. Rep. **407**, 205 (2005).
[15] M. G. Alford, A. Schmitt, K. Rajagopal, and T. Schäfer, Rev. Mod. Phys. **80**, 1455 (2008).
[16] M. Asakawa and K. Yazaki, Nucl. Phys. **A504**, 668 (1989).
[17] A. Barducci, R. Casalbuoni, S. De Curtis, R. Gatto, and G. Pettini, Phys. Lett. B **231**, 463 (1989).
[18] T. Kunihiro, Nucl. Phys. **B351**, 593 (1991).
[19] J. Berges and K. Rajagopal, Nucl. Phys. **B538**, 215 (1999).
[20] S. B. Ruester, V. Werth, M. Buballa, I. A. Shovkovy, and D. H. Rischke, Phys. Rev. D **72**, 034004 (2005).
[21] H. Abuki and T. Kunihiro, Nucl. Phys. **A768**, 118 (2006).
[22] As a review, see, M. A. Stephanov, Prog. Theor. Phys. Suppl. **153**, 139 (2004); Int. J. Mod. Phys. A **20**, 4387

(2005); Proc. Sci., LAT2006 (2006) 024 [arXiv:hep-lat/0701002].
[23] M. A. Stephanov, K. Rajagopal, and E. V. Shuryak, Phys. Rev. Lett. **81**, 4816 (1998).
[24] Y. Minami and T. Kunihiro, Prog. Theor. Phys. **122**, 881 (2009).
[25] E. S. Bowman and J. I. Kapusta, Phys. Rev. C **79**, 015202 (2009).
[26] L. Ferroni, V. Koch, and M. B. Pinto, Phys. Rev. C **82**, 055205 (2010).
[27] M. Kitazawa, T. Koide, T. Kunihiro, and Y. Nemoto, Prog. Theor. Phys. **108**, 929 (2002).
[28] M. Kitazawa, T. Koide, T. Kunihiro, and Y. Nemoto, Prog. Theor. Phys. **110**, 185 (2003).
[29] Z. Zhang, K. Fukushima, and T. Kunihiro, Phys. Rev. D **79**, 014004 (2009).
[30] Z. Zhang and T. Kunihiro, Phys. Rev. D **80**, 014015 (2009).
[31] N. Evans, S. D. H. Hsu and M. Schwetz, Nucl. Phys. **B551**, 275 (1999).
[32] T. Schäfer and F. Wilczek, Phys. Lett. B **450**, 325 (1999).
[33] M. Huang and I. A. Shovkovy, Phys. Rev. D **70**, 094030 (2004); **70**, 094030 (2004).
[34] R. Rapp, T. Schafer, E. V. Shuryak, and M. Velkovsky, Ann. Phys. (N.Y.) **280**, 35 (2000).
[35] A. W. Steiner, Phys. Rev. D **72**, 054024 (2005).
[36] T. Hatsuda, M. Tachibana, N. Yamamoto, and G. Baym, Phys. Rev. Lett. **97**, 122001 (2006).
[37] N. Yamamoto, M. Tachibana, T. Hatsuda, and G. Baym, Phys. Rev. D **76**, 074001 (2007).
[38] G. Baym, T. Hatsuda, M. Tachibana, and N. Yamamoto, J. Phys. G **35**, 104021 (2008).
[39] H. Abuki, G. Baym, T. Hatsuda, and N. Yamamoto, Phys. Rev. D **81**, 125010 (2010).
[40] H. Basler and M. Buballa, Phys. Rev. D **82**, 094004 (2010).
[41] M. G. Alford, K. Rajagopal, and F. Wilczek, Phys. Lett. B **422**, 247 (1998).
[42] R. Rapp, T. Schäfer, E. V. Shuryak, and M. Velkovsky, Phys. Rev. Lett. **81**, 53 (1998).
[43] I. Giannakis and H. C. Ren, Phys. Lett. B **611**, 137 (2005).
[44] E. V. Gorbar, M. Hashimoto, and V. A. Miransky, Phys. Lett. B **632**, 305 (2006); Phys. Rev. Lett. **96**, 022005 (2006); Phys. Rev. D **75**, 085012 (2007).
[45] O. Kiriyama, Phys. Rev. D **74**, 114011 (2006).
[46] L. He, M. Jin, and P. Zhuang, Phys. Rev. D **75**, 036003 (2007).
[47] K. Fukushima, Phys. Rev. D **72**, 074002 (2005).
[48] M. Kitazawa, D. H. Rischke, and I. A. Shovkovy, Phys. Lett. B **637**, 367 (2006).
[49] S. Klimt, M. Lutz, U. Vogl, and W. Weise, Nucl. Phys. **A516**, 429 (1990).
[50] T. Kunihiro, Phys. Lett. B **271**, 395 (1991).
[51] M. Kobayashi and T. Maskawa, Prog. Theor. Phys. **44**, 1422 (1970).
[52] G. 't Hooft, Phys. Rev. D **14**, 3432 (1976); **18**, 2199(E) (1978); Phys. Rep. **142**, 357 (1986).
[53] T. Kunihiro, Phys. Lett. B **219**, 363 (1989).
[54] W. j. Fu, Z. Zhang, and Y. x. Liu, Phys. Rev. D **77**, 014006 (2008).
[55] T. Kunihiro, Prog. Theor. Phys. **122**, 255 (2009).
[56] S. Weinberg, Phys. Rev. D **11**, 3583 (1975).
[57] T. Schäfer and E. Shuryak, Rev. Mod. Phys. **70**, 323 (1998).
[58] P. Rehberg, S. P. Klevansky, and J. Hufner, Phys. Rev. C **53**, 410 (1996).
[59] M. Alford and K. Rajagopal, J. High Energy Phys. 06 (2002) 031; A. W. Steiner, S. Reddy, and M. Prakash, Phys. Rev. D **66**, 094007 (2002).
[60] E. Nakano and T. Tatsumi, Phys. Rev. D **71**, 114006 (2005).
[61] D. Nickel, Phys. Rev. Lett. **103**, 072301 (2009).
[62] D. Nickel, Phys. Rev. D **80**, 074025 (2009).
[63] S. Carignano, D. Nickel, and M. Buballa, Phys. Rev. D **82**, 054009 (2010).
[64] I. Shovkovy and M. Huang, Phys. Lett. B **564**, 205 (2003); M. Huang and I. Shovkovy, Nucl. Phys. **A729**, 835 (2003).
[65] C. D. Roberts and A. G. Williams, Prog. Part. Nucl. Phys. **33**, 477 (1994); P. C. Tandy, Prog. Part. Nucl. Phys. **39**, 117 (1997).
[66] K.-I. Aoki, Int. J. Mod. Phys. B **14**, 1249 (2000).
[67] J. Berges, N. Tetradis, and C. Wetterich, Phys. Rep. **363**, 223 (2002).